PHYSICAL REVIEW E VOLUME 50, NUMBER 2 AUGUST 1994

Some simple chaotic flows

J. C. Sprott*
Department of Physics, University of Wisconsin, Madison, Wisconsin 53706
(Received 17 January 1994)

A systematic examination of general three-dimensional autonomous ordinary differential equations with quadratic nonlinearities has uncovered 19 distinct simple examples of chaotic flows with either five terms and two nonlinearities or six terms and one nonlinearity. The properties of these systems are described, including their critical points, Lyapunov exponents, and fractal dimensions.

PACS number(s): 05.45.+b, 47.52.+j, 02.60.Cb, 02.30.Hq

One remarkable feature of chaos is that it can occur in very simple low-dimensional nonlinear equations. The Poincaré-Bendixson theorem [1] requires that autonomous first-order ordinary differential equations (ODE's) with continuous functions be at least three dimensional to have bounded chaotic solutions. Two standard examples are the Lorenz [2], $\dot{x}=-\sigma x+\sigma y$, $\dot{y}=rx-xz-y$, $\dot{z}=xy-bz$, and Rössler [3] systems, $\dot{x}=-y-z$, $\dot{y}=x+ay$, $\dot{z}=b+xz-cz$. These cases are characterized by seven terms and either two quadratic nonlinearities or one quadratic nonlinearity, respectively.

It is interesting to ask whether there are systems of autonomous ordinary differential equations with one or two quadratic nonlinearities and fewer than seven terms whose solutions are chaotic. Such cases would in some sense be simpler than the Lorenz and Rössler equations and would challenge Lorenz's claim that Rössler's example is the simplest known chaotic flow [4]. The simplicity refers to the algebraic representation rather than to the physical process described by the equations. Such equations would be of mathematical and practical interest. For example, it has been proposed that chaotic electrical circuits could be used for real-time enciphering and deciphering of speech for secure communications [5,6]. An appropriate system could be chosen from a catalog of simple chaotic equations to optimize factors such as robustness to errors in the parameters and immunity to noise.

Consider general three-dimensional ODE's with quadratic nonlinearities of the form $\dot{\mathbf{x}}=\mathbf{a}+\sum_{i=1}^{3}\mathbf{b}_i\mathbf{x}_i+\sum_{i=1}^{3}\sum_{j=i}^{3}\mathbf{c}_{i,j}\mathbf{x}_i\mathbf{x}_j$, where $\mathbf{x}=(x,y,z)$ is a real three-dimensional state-space variable, and $\mathbf{a}$, $\mathbf{b}$, and $\mathbf{c}$ are real three-dimensional coefficient vectors. The numerical procedure [7] was to search hyperplanes of six or fewer dimensions in the 30-dimensional control space of coefficients for bounded chaotic solutions as evidenced by a positive Lyapunov exponent [8]. The calculations were performed using a fourth-order Runge-Kutta integrator with a step size of $\Delta t=0.01$.

The six (or fewer) nonzero coefficients were assigned values in the range -5 to 5 in increments of 0.1, giving the order of 10^{20} cases, of which about 10^8 were randomly chosen for examination. Note that the coefficient range can be chosen arbitrarily since time can be rescaled. Several thousand chaotic cases were found, 33 of which are distinct in the sense that their functional forms are different and not related by a trivial transposition of variables. By performing various algebraic transformations on these cases, 15 additional cases were found that satisfy the above criterion of simplicity. Of the 48 total cases, only 19 appear to be distinct in the sense that there is no obvious transformation of one to another. For each case, as many of the coefficients were set to ± 1 as possible. It is generally possible to normalize four of the coefficients by rescaling each of the four variables (x, y, z, and t). Consequently, equations with six or fewer terms have at most two independent control parameters.

The nineteen distinct cases are shown in Table I. Cases A–E have five terms and two nonlinearities, while cases F–S have six terms and one nonlinearity. Many cases with six terms and two nonlinearities were found, but they are more complicated than these cases and hence are not listed. No cases were found with five terms and one nonlinearity or with fewer than five terms and any number of (quadratic) nonlinearities. Case A is a volume-conserving system, and the others are dissipative systems with strange attractors. Initial conditions of $x=y=z=0.05$ suffice for the attractors, and a chaotic solution for case A is obtained, for example, with initial conditions of $\mathbf{x}=(0,5,0)$.

Figure 1 shows a Poincaré section for case A in which points are plotted where the trajectory punctures the $z=0$ plane for various initial conditions. The quasiperiodic orbits are surrounded by a chaotic region. This case has no critical points (where $\dot{\mathbf{x}}=\mathbf{0}$), although there are periodic orbits.

The (x,y,z) coordinates of all the critical points are given in Table I. The linear stability of each critical point was determined by calculating the eigenvalues of the linearized Jacobian matrix. Most cases have one real eigenvalue and a complex-conjugate pair (a so-called saddle focus). Case L has three real eigenvalues (a so-called saddle node). Such saddle points admit homoclinic orbits for certain values of the parameters near which chaos results [9].

The complex cases are denoted in Table I by c (center) if the real part is zero or f (focus) if the real part is nonzero. The saddle node (case L) is indicated by n. The digit following c, f, or n is the instability index (the number of eigenvalues with a positive real part, or, equivalently, the dimension of the unstable manifold or "outset"). Those cases with an index of zero are neutrally linearly stable (they have ei-

*Electronic address: sprott@juno.physics.wisc.edu

TABLE I. Algebraically simple three-dimensional ODE's with chaotic solutions.

Case	Equations	Critical points	Lyapunov exponents	Dimension
A	$\dot{x}=y$ $\dot{y}=-x+yz$ $\dot{z}=1-y^2$	none	0.014 0 −0.014	3.000
B	$\dot{x}=yz$ $\dot{y}=x-y$ $\dot{z}=1-xy$	$f2(1,1,0)$ $f2(-1,-1,0)$	0.210 0 −1.210	2.174
C	$\dot{x}=yz$ $\dot{y}=x-y$ $\dot{z}=1-x^2$	$c0(1,1,0)$ $c0(-1,-1,0)$	0.163 0 −1.163	2.140
D	$\dot{x}=-y$ $\dot{y}=x+z$ $\dot{z}=xz+3y^2$	$c0(0,0,0)$	0.103 0 −1.320	2.078
E	$\dot{x}=yz$ $\dot{y}=x^2-y$ $\dot{z}=1-4x$	$c0(0.25,0.063,0)$	0.078 0 −1.078	2.072
F	$\dot{x}=y+z$ $\dot{y}=-x+0.5y$ $\dot{z}=x^2-z$	$f2(0,0,0)$ $f1(-2,-4,4)$	0.117 0 −0.617	2.190
G	$\dot{x}=0.4x+z$ $\dot{y}=xz-y$ $\dot{z}=-x+y$	$f2(0,0,0)$ $f1(-2.5,-2.5,1)$	0.034 0 −0.634	2.054
H	$\dot{x}=-y+z^2$ $\dot{y}=x+0.5y$ $\dot{z}=x-z$	$f2(0,0,0)$ $f2(-2,4,-2)$	0.117 0 −0.617	2.190
I	$\dot{x}=-0.2y$ $\dot{y}=x+z$ $\dot{z}=x+y^2-z$	$f2(0,0,0)$	0.012 0 −1.012	2.012
J	$\dot{x}=2z$ $\dot{y}=-2y+z$ $\dot{z}=-x+y+y^2$	$f2(0,0,0)$	0.076 0 −2.076	2.037
K	$\dot{x}=xy-z$ $\dot{y}=x-y$ $\dot{z}=x+0.3z$	$f2(0,0,0)$ $f1(-3.333,-3.333,11.111)$	0.038 0 −0.890	2.042
L	$\dot{x}=y+3.9z$ $\dot{y}=0.9x^2-y$ $\dot{z}=1-x$	$n1(1,1.111,-0.231)$	0.061 0 −1.061	2.057
M	$\dot{x}=-z$ $\dot{y}=-x^2-y$ $\dot{z}=1.7+1.7x+y$	$f1(2.406,-5.791,0)$ $f2(-0.706,-0.499,0)$	0.044 0 −1.044	2.042
N	$\dot{x}=-2y$ $\dot{y}=x+z^2$ $\dot{z}=1+y-2z$	$f2(-0.25,0,0.5)$	0.076 0 −2.076	2.037
O	$\dot{x}=y$ $\dot{y}=x-z$ $\dot{z}=x+xz+2.7y$	$f1(0,0,0)$ $f0(-1,0,-1)$	0.049 0 −0.319	2.154
P	$\dot{x}=2.7y+z$ $\dot{y}=-x+y^2$ $\dot{z}=x+y$	$f2(0,0,0)$ $f2(1,-1,2.7)$	0.087 0 −0.481	2.181
Q	$\dot{x}=-z$ $\dot{y}=x-y$ $\dot{z}=3.1x+y^2+0.5z$	$f2(0,0,0)$ $f1(-3.1,-3.1,0)$	0.109 0 −0.609	2.179
R	$\dot{x}=0.9-y$ $\dot{y}=0.4+z$ $\dot{z}=xy-z$	$f2(-0.444,1.111,-0.4)$	0.062 0 −1.062	2.058
S	$\dot{x}=-x-4y$ $\dot{y}=x+z^2$ $\dot{z}=1+x$	$f2(-1,0.25,1)$ $f1(-1,0.25,-1)$	0.188 0 −1.188	2.151

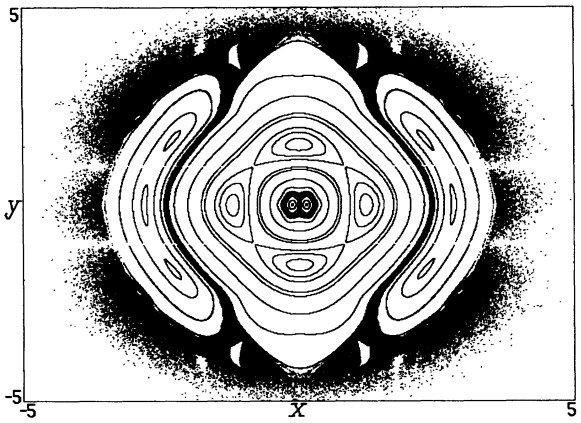

FIG. 1. Poincaré section at $z=0$ for the conservative chaotic case A in Table I.

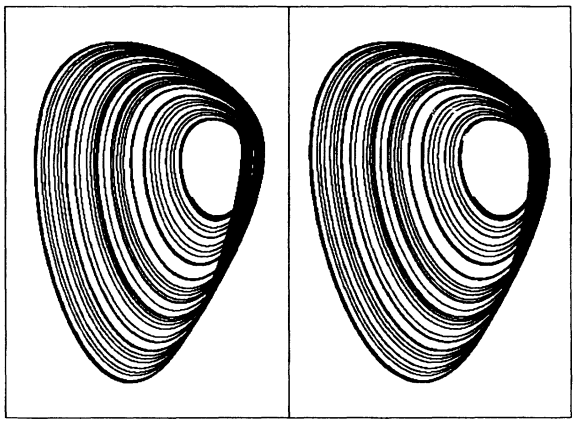

FIG. 3. Stereoscopic plot of the trajectory for the case N chaotic attractor in Table I.

genvalues whose real part is zero), but they are nonlinearly unstable with a saddle point, as must be the case with quadratic nonlinearities.

Cases B and C resemble the Lorenz attractor in that they have two symmetrical critical points (at $x=y=\pm 1$, $z=0$). However, the origin is not a critical point as it is for the Lorenz attractor, but rather it has a strong uniform flow in the $+z$ direction. Figure 2 shows a stereoscopic plot of the trajectory for case B. Case C is similar except that the orbit spirals outward more slowly because the critical points are only weakly unstable. In these stereoscopic plots, you are looking down on the xy plane from the $+z$ axis. Cases D–S all have similar structure and topologically resemble the Rössler attractor in that they are dominated by a single folded band. Case N is typical and is shown in Fig. 3 as a stereoscopic plot.

The three Lyapunov exponents were calculated numerically for each case. The largest exponent is positive as required for chaos. Indeed this is the criterion whereby chaotic solutions were identified. The procedure was to perturb the initial condition in an arbitrary direction by a small displacement ε_0 and calculate the separation ε_1 after one iteration time step Δt. The perturbed orbit was then readjusted after each time step back to a separation of ε_0 along the direction of the separation. The largest Lyapunov exponent was calculated from $\lambda_1=\langle \ln(\varepsilon_1/\varepsilon_0)\rangle/\Delta t$, where the brackets denote an average over at least 10^8 iterations (total time of 10^6), and ε_0 was taken as 10^{-8}. The first 32 000 iterations were discarded to ensure that the orbit was on the attractor and that the separation was along the direction of fastest growth. The calculation was done in extended (80-bit) precision, and it was verified that the result is not sensitive to ε_0, Δt, initial conditions, or the number of iterations. The long calculation time helps ensure that the solutions are steady states rather than chaotic transients. The procedure was tested with the Lorenz attractor. Note that the exponents are base e rather than base 2 as is sometimes used [10].

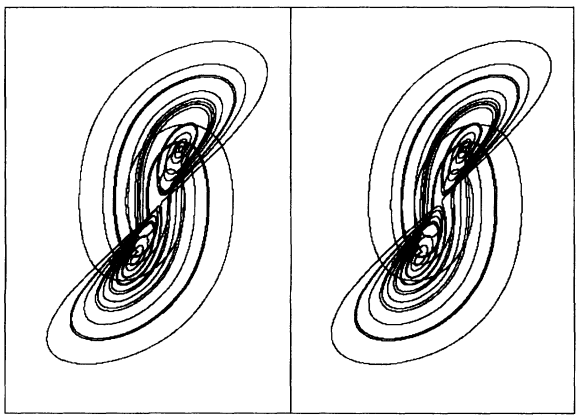

FIG. 2. Stereoscopic plot of the trajectory for the case B chaotic attractor in Table I.

Continuous flows necessarily have a zero Lyapunov exponent ($\lambda_2=0$) corresponding to the direction of the flow. The third exponent λ_3 must be negative for a conservative or dissipative system. The sum of the three exponents is the average rate of fractional volume expansion along the trajectory, and it is easily calculated from the trace of the Jacobian matrix J, which is the divergence of the flow:

$$\frac{1}{V}\frac{dV}{dt}=\mathrm{Tr}J=\frac{\partial \dot{x}}{\partial x}+\frac{\partial \dot{y}}{\partial y}+\frac{\partial \dot{z}}{\partial z}=\lambda_1+\lambda_2+\lambda_3.$$

This quantity is constant for most of the cases in Table I. The exceptions are cases A, D, K, O, and P. For those cases, the average value of TrJ along the trajectory was calculated numerically to determine the average rate of volume contraction. The Lyapunov exponents are given in Table I. All digits are significant.

From the spectrum of Lyapunov exponents, the Lyapunov dimension can be calculated from $D_L=2-\lambda_1/\lambda_3$. It has been conjectured [11] that D_L is the same as the information dimension for typical attractors. Values of D_L are given in Table I.

The capacity dimension [12] and correlation dimension [13] were calculated for each case. They were found to agree with the Lyapunov dimension with a root-mean-squared error of about 6%. However, the values are much less certain than the Lyapunov dimension and may be subject to system-

atic errors. Consequently, these other dimensions are not reported here but will be the subject of further study.

The basins of attraction have not been examined in detail for the various cases. However, a very large sphere (radius 10^6) was constructed around each attractor, and the fraction of the area of the sphere for which the flow vector is outward was calculated for each case. In most cases the result was 50%. The exceptions are case A, where it is 100%, and case B, where it is 32%. Thus it appears that none of the cases attracts the entire state space.

Time was also run backward for each case beginning with an initial condition on the attractor. The resulting orbit was unbounded for all the dissipative cases, escaping in a few thousand iterations, confirming that the attractive basin extends to infinity in at least one direction for each case. The only exception is case A, whose time-reversal invariance is evident from the equations.

For each case, at least one parameter in the equations was varied over the range -5 to $+5$ in small steps to test the robustness of the solution to small parameter changes and to look for evidence of riddled parameter space [14]. In each case the largest Lyapunov exponent is positive and smoothly varying in the vicinity of the value listed in Table I. For some cases, the window of chaotic behavior is very narrow, and the Lyapunov exponent changes rapidly but smoothly within the window. A common circumstance is for the chaotic region to be sandwiched between regions of periodic solutions ($\lambda_1=0$) and unbounded solutions and to have embedded windows of periodicity. Case B with the 1 in the $\dot{z}$ equation replaced by a constant in the range of -1 to -2 has limit-cycle solutions riddled with stable critical-point solutions. Over most of this range the largest Lyapunov exponent λ_1 fluctuates from zero to a large negative value for very small ($<10^{-16}$) parameter changes with what appears to be self-similar structure. Other cases show similar examples of such riddling but over smaller ranges of their parameters.

It is interesting to ask how the chaotic solutions are distributed throughout the 30-dimensional control space. With only a few thousand samples distributed along five-dimensional (5D) or 6D hyperplanes, it is difficult to draw general conclusions. However, a previous, more extensive study [15] involving about 35 000 chaotic cases showed them to be clustered in a region whose fractal boundary has a dimension about half the dimension of the space. In that study, three-dimensional ODE's with general quadratic nonlinearities had bounded solutions over about 20% of the control space and chaotic solutions over about 0.1% of the space. For the cases studied here, the fraction of bounded solutions ranges from about 10% to 30%, and the fraction of chaotic solutions ranges from about 0.03% (for case S) to about 3% (for case B). The attractors with five terms (cases B–E) and those with six terms (cases F–S), respectively, are arranged in Table I approximately in descending order of the probability of their having chaotic solutions for randomly chosen coefficients.

The method employed cannot guarantee that these are the simplest chaotic systems of ODE's or that all the chaotic systems of three-dimensional ODE's with five terms and two quadratic nonlinearities or with six terms and one quadratic nonlinearity have been discovered. However, the cases with five terms appeared early and often in the search, and it is likely they have all been found. New cases with six terms were still occasionally being found when the search was terminated after about 2000 h of computing, and thus additional such cases probably exist. Furthermore, because of the tedious calculations required to test algebraic equivalence, it is possible that some of the cases listed in the table are not distinct. The algebraic simplicity of these systems should invite further detailed study, and they might serve as better examples than the ones invariably used to illustrate chaotic flows.

I am grateful to Adam Fleming for independently calculating the Lyapunov exponents and for numerous stimulating discussions.

[1] M. W. Hirsch and S. Smale, *Differential Equations, Dynamical Systems and Linear Algebra* (Academic, New York, 1974).
[2] E. N. Lorenz, J. Atmos. Sci. **20**, 130 (1963).
[3] O. E. Rössler, Phys. Lett. **57A**, 397 (1976).
[4] E. N. Lorenz, *The Essence of Chaos* (University of Washington Press, Seattle, 1993), p. 148.
[5] S. Hayes, C. Grebogi, and E. Ott, Phys. Rev. Lett. **70**, 3031 (1993).
[6] K. M. Cuomo and A. V. Oppenheim, Phys. Rev. Lett. **71**, 65 (1993).
[7] J. C. Sprott, Comput. Graphics **7**, 325 (1993).
[8] G. Benettin, L. Galgani, A. Giorgilli, and J.-M. Strelcyn, Meccanica **15**, 21 (1980).
[9] L. P. Shilnikov, Math. USSR Sbornik **10**, 91 (1970).
[10] A. Wolf, J. B. Swift, H. L. Swinney, and J. A. Vastano, Physica D **16**, 285 (1985).
[11] J. L. Kaplan and J. A. Yorke, in *Functional Differential Equations and Approximations of Fixed Points*, edited by H.-O. Peitgen and H.-O. Walter, Lecture Notes in Mathematics Vol. 730 (Springer, Berlin, 1979), p. 204.
[12] J. D. Farmer, E. Ott, and J. A. Yorke, Physica D **7**, 153 (1983).
[13] P. Grassberger and I. Procaccia, Phys. Rev. Lett. **50**, 346 (1983).
[14] Y. C. Lai and R. L. Winslow, Phys. Rev. Lett. **72**, 1640 (1994).
[15] J. C. Sprott, Phys. Lett. A **173**, 21 (1993).

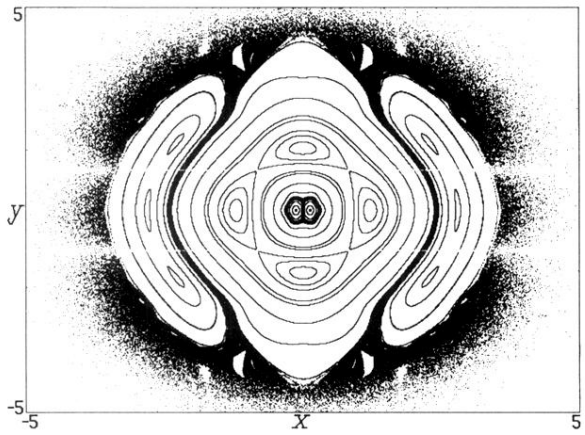

FIG. 1. Poincaré section at $z=0$ for the conservative chaotic case A in Table I.

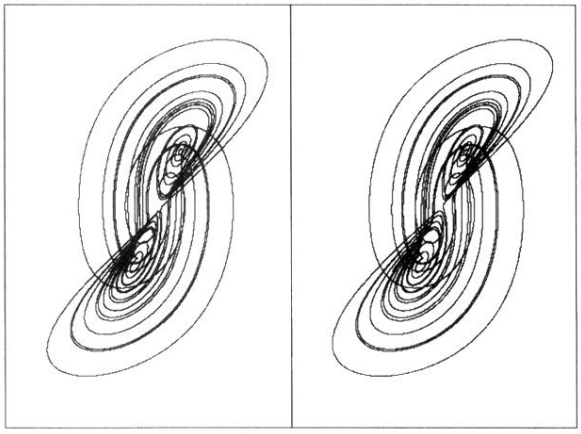

FIG. 2. Stereoscopic plot of the trajectory for the case B chaotic attractor in Table I.

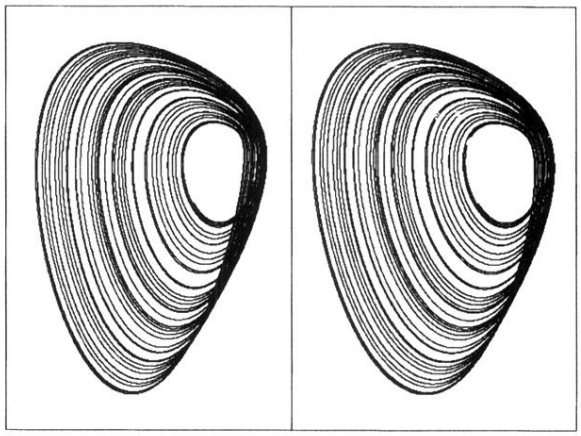

FIG. 3. Stereoscopic plot of the trajectory for the case N chaotic attractor in Table I.